Identification and functional characterization of rare mutations of the neuroligin-2 gene (*NLGN2*) associated with schizophrenia

Chicheng Sun [1],[†], **Min-Chih Cheng** [2],[†], **Rosie Qin** [1], **Ding-Lieh Liao** [3], **Tzu-Ting Chen** [2], **Farn-Jong Koong** [4], **Gong Chen** [1],[‡] **and Chia-Hsiang Chen** [5],[6],[7],[*]

[1]Department of Biology, The Huck Institutes of Life Sciences, The Pennsylvania State University, University Park, PA, USA, [2]Department of Psychiatry, Yuli Mental Health Research Center, Yuli Veterans Hospital, Hualien, Taiwan, Republic of China [3]Department of Health, Bali Psychiatric Center, Executive Yuan, Taipei, Taiwan, Republic of China [4]Department of Health, Yuli General Hospital, Executive Yuan, Taipei, Taiwan, Republic of China [5]Division of Mental Health and Addiction Medicine, National Health Research Institutes, Zhunan Town, Miaoli County 350, Taiwan, Republic of China [6]Department of Psychiatry, Chang Gung Memorial Hospital at Linkou and Chang Gung University School of Medicine, Taoyuan, Taiwan, Republic of China and [7]Institute of Medical Sciences, Tzu-Chi University, Hualien, Taiwan, Republic of China

Schizophrenia is a severe chronic mental disorder with a high genetic component in its etiology. Several lines of study have suggested that synaptic dysfunction may underlie the pathogenesis of schizophrenia. Neuroligin proteins function as cell-adhesion molecules at post-synaptic membrane and play critical roles in synaptogenesis and synaptic maturation. In this study, we systemically sequenced all the exons and promoter region of neuroligin-2 (*NLGN2*) gene in a sample of 584 schizophrenia patients and 549 control subjects from Taiwan. In total, we identified 19 genetic variants, including six rare missense mutations such as R215H (one patient), V510M (two patients), R621H (one patient), A637T (two patients), P800L (one patient and one control) and A819S (one patient and one control). *In silico* analysis predicted that two patient-specific missense mutations, R215H and R621H, had damaging effect, whereas the other missense mutations were benign. Importantly, functional analysis with immunocytochemistry and electrophysiological recordings identified the R215H mutant as a loss-of-function mutant in inducing GABAergic synaptogenesis. Mechanistically, the synaptogenic deficiency of R215H mutant was due to its retention inside the endoplasmic reticulum and inability to be transported to cell membrane. Our study suggests that defects in GABAergic synapse formation in the brain may be an important contributing factor for the onset of schizophrenia. In the family study of this mutation, we found his elder brother also carried this mutation but did not have psychiatric symptoms, indicating that this mutation has incomplete penetrance, and thus the clinical relevance of this mutation should be interpreted with caution.

INTRODUCTION

Schizophrenia is a severe chronic mental disease that affects ~1% of the general population worldwide. The onset of schizophrenia usually starts from adolescence and young adulthood, and the symptoms of schizophrenia include both positive symptoms (delusion, hallucination, disorganized thinking and bizarre behavior) and negative symptoms (poverty of speech, avolition, social withdrawal and blunt

affect). Genetic epidemiological studies, highlighted by twin studies, have demonstrated that schizophrenia is a complex disorder with high heritability (1). Specifically, previous studies indicate that synaptic dysfunction is involved in the pathogenesis of schizophrenia and patients with schizophrenia also have synaptic degeneration in the brain (2,3). Therefore, genes involved in the formation and functional integrity of synapses may be potential candidate genes of schizophrenia.

Post-synaptic neuroligins (NLGNs) and presynaptic neurexins (NRXNs) are among the most well-characterized synaptic cell-adhesion molecules that are capable of promoting both excitatory and inhibitory synapse formation. Because of their large number of splicing isoforms, it has been proposed that selective binding between NLGNs and NRXNs could function as synaptic code in guiding the neural network formation (4). In human, there are five *NLGN* genes with *NLGN1/2* located on autosomes and *NLGN3/4/4Y* on sex chromosomes. NLGN1 and NLGN2 are the two highly expressed and mostly studied isoforms and are essential for excitatory and inhibitory synaptic functions, respectively (5,6). Besides mediating the adhesion between pre- and post-synaptic membranes, the NLGN–NRXN complex has also been shown to regulate the pre-synaptic release of neurotransmitters and synaptic plasticity (7–9). The critical function of NLGN and NRXN during neural development is underlined by recent discovery of mutations in *NRXN1*, *NLGN3* and *NLGN4* genes in patients with autism (4,10), a childhood-onset mental disease characterized by impaired reciprocal social interaction and language development and the presence of restricted interest and compulsive behavior.

There are overlapping symptoms between schizophrenia and autism, especially the negative symptoms (11,12), which may suggest that these two diseases share some common biological basis in their pathogenesis. In fact, mutations in *NRXN1* and *NLGN4* genes have also been found in schizophrenia patients (13–16). Among NLGN family proteins, NLGN2 is critical for inhibitory synaptic transmission (6) and defects in inhibitory circuit function contribute to the working memory impairments that represent major clinical features of schizophrenia (17). In this study, we investigated whether mutations in the *NLGN2* gene are associated with schizophrenia by systemically screening for mutations in the exon and promoter region of *NLGN2* in a cohort of schizophrenia patients. As a result, we identified six rare missense point mutations in the *NLGN2* gene in this cohort, including R215H, V510M, R621H, A637T, P800L and A819S. Importantly, functional analysis in a molecularly engineered GABAergic synapse model revealed R215H as a loss-of-function mutation. Unlike the wild-type protein, the NLGN2 mutant R215H was found to be incapable of inducing GABAergic synapse formation due to a severe defect in intracellular trafficking. Thus, disrupting normal GABAergic circuit formation may be one of the important etiologies for schizophrenia.

RESULTS

Identification of six rare missense mutations of NLGN2 gene

Following the systemic sequencing of all the exons and the promoter region of *NLGN2* gene in 584 schizophrenia patients and 549 control subjects, we totally identified 19 genetic

variants in this sample. The positions of these variants are illustrated in Figure 1A. Notably, among these 19 variants, six were novel missense mutations that were not reported before in the literature, including a G-to-A substitution (c.644G > A) at codon 215 (R215H) in one schizophrenia patient; a G-to-A substitution (c.1528G > A) at codon 510 (V510M) in two patients; a G-to-A substitution (c.1862G > A) at codon 621 (R621H) in one patient; a G-to-A substitution (c.1909G > A) at codon 637 (A637T) in two patients; a C-to-T substitution (c.2399C > T) at codon 800 (P800L) in one patient and one control subject and a G-to-T substitution (c.2455G > T) at codon 819 (A819S) in one patient and one control subject. The sequencing data are shown in Figure 1B. Two missense mutations (R215H and V510M) were further verified using restriction fragment length polymorphism (RFLP) as illustrated in Figure 1C. Protein sequence alignments of all human NLGNs surrounding mutant sites are shown in Figure 1D. Amino acids R215, V510, R621 and A637 are located at the extracellular domain of NLGN2, while P800 and A819 are at the intracellular terminal. *In silico* analysis of these six missense variants predicted two missense mutations, R215H and R621H, as of probable damaging, while the other four missense mutations being benign (Table 1). Because mutants P800L and A819S also appeared in control subjects, we focused on schizophrenia patient-specific mutants, R215H, V510M, R621H and A637T, in our functional characterization studies.

The R215H mutant was impaired in mediating heterophilic cell adhesion

We first tested the ability of NLGN2 mutants in mediating cell adhesion through binding with their receptor NRXN1β. In cell aggregation assay as shown in Figure 2, NRXN1β-expressing HEK 293T cells form large cell aggregates with wild-type NLGN2-expressing cells (Fig. 2A). However, NRXN1β-expressing cells did not aggregate with GFP-expressing cells (Fig. 2B), indicating that the observed cell aggregation was mediated by the specific NLGN2–NRXN1β interaction, not by other endogenous cell-adhesion molecules in HEK 293T cells. In the assay of four NLGN2 mutants, R215H-expressing cells had significantly reduced aggregates with NRXN1β-expressing cells (Fig. 2C), while the other three mutants did not show significant differences in forming cell aggregates when compared with the wild-type NLGN2 (Fig. 2D–F). Quantitative analysis confirmed that the R215H mutant, but not the other three mutants, has significantly reduced aggregation index when compared with the wild-type NLGN2 ($P < 0.01$, Fig. 2G). Together, these data suggest that the R215H mutant has severe impairment in mediating heterophilic cell adhesion.

The R215H mutant could not induce pre-synaptic differentiation

Previously, we have shown that NLGN2 promotes GABAergic synapse formation in HEK 293T-neuron co-culture system (18). Using this model system, we examined the synaptogenic potency of the four NLGN2 mutants. Immunostaining of glutamic acid decarboxylase (GAD), a pre-synaptic marker for GABAergic terminals, was conducted to assess the extent of
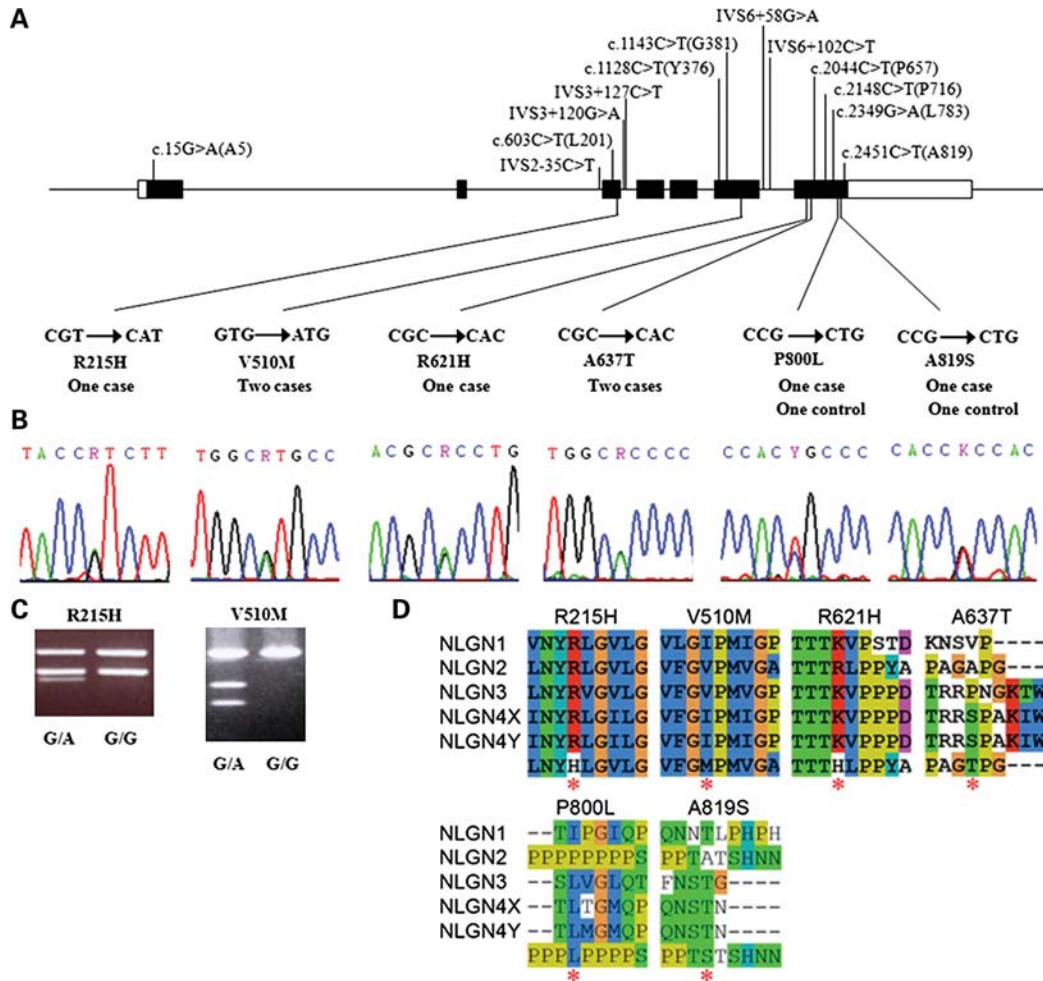
Figure 1. Genetic variants of the *NLGN2* identified in this study. (**A**) Distributions of the 19 variants of the *NLGN2* gene found in this study, including six missense mutations. (**B**) Sequence electropherograms of six missense mutations of the *NLGN2* gene identified in this study. (**C**) PCR-based RFLP analysis for the genotyping of R215H and V510M. (**D**) Protein sequence alignments of all the human NLGNs surrounding mutant sites (generated by Clustal X2 software, http://www.clustal.org/). Red asterisks indicate missense mutations identified in this study.

Table 1. *In silico* analysis of six missense mutations of the *NLGN2* gene identified in this study

Mutation in cDNA	Amino acid change	Predicted deleterious PolyPhen-2[a]	SIFT[b]
c.644G > A	R215H	Probably damaging	Affect protein function
c.1528G > A	V510M	Benign	Tolerated
c.1862G > A	R621H	Possibly damaging	Affect protein function
c.1909G > A	A637T	Benign	Tolerated
c.2399C > T	P800L	Benign	Tolerated
c.2455C > T	A819S	Benign	Tolerated

[a]PolyPhen-2: http://genetics.bwh.harvard.edu/pph2/
[b]SIFT: http://sift.jcvi.org/

GABAergic innervation onto NLGN2-expressing HEK 293T cells. The R215H mutant showed no GAD positive cell out of 27 cells examined, while the wild-type NLGN2 and the other three mutants showed comparable percentage of GAD positive cells (Fig. 3). Thus, consistent with the lack of cell

adhesion ability, the R215H mutant is deficient in promoting GABAergic pre-synaptic differentiation.

The R215H mutant showed defective synaptogenic function

In corroborating with morphological analysis, whole-cell patch clamp recordings were employed to investigate spontaneous GABAergic inhibitory post-synaptic currents (IPSCs) in HEK cells co-transfected with NLGN2 and GABA$_A$Rs (18). Wild-type NLGN2 induced robust IPSCs in co-cultured HEK cells that were completely blocked by GABA$_A$R antagonist bicuculline (Fig. 4A). Brief application of GABA (100 μM) resulted in significant whole-cell GABA currents in transfected HEK 293T cells, indicating the surface expression of functional GABA$_A$Rs (Fig. 4A). Consistent with the GAD staining data, the R215H mutant was significantly less potent than the wild-type NLGN2 in inducing GABAergic events in co-cultured HEK 293T cells (Fig. 4B). As the wild-type NLGN2 induced IPSCs in 64 ± 8% of transfected HEK 293T cells ($n = 33$), the R215H mutant only
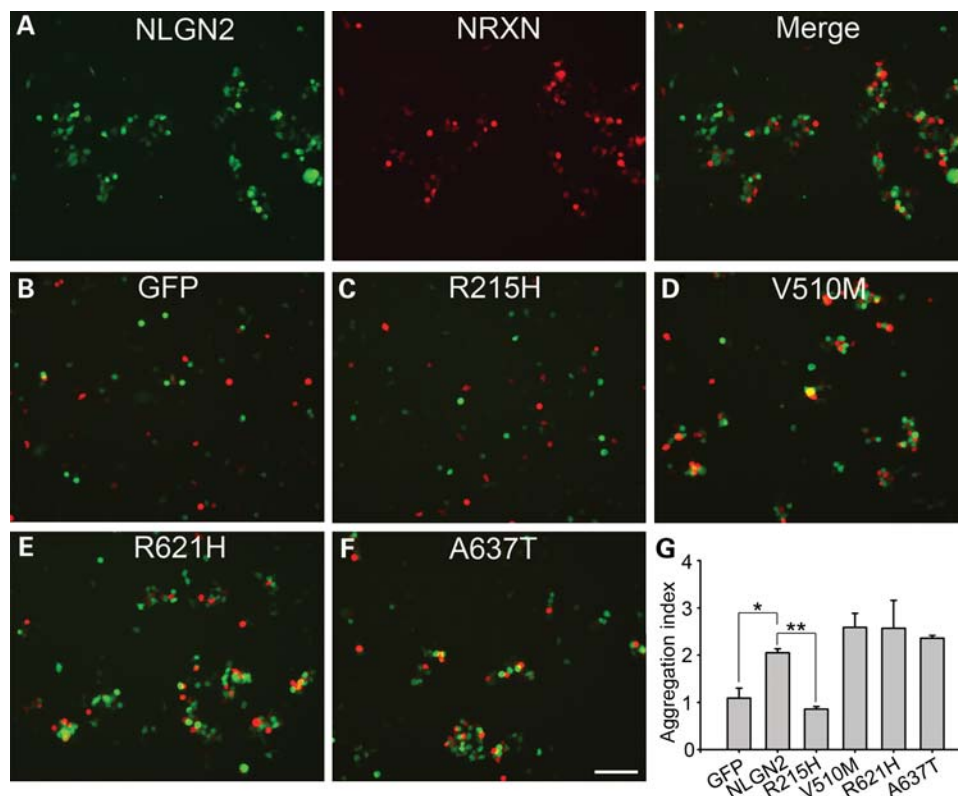
Figure 2. Lack of interaction between R215H mutant and NRXN-expressing HEK 293T cells. (**A**) Cells expressing the wild-type NLGN2 (green) were mixed with cells expressing NRXN1β (Red), and merged image showed the aggregation of NLGN2-expressing and NRXN1β-expressing HEK 293T cells. (**B**) GFP-expressing and NRXN-expressing HEK 293T cells did not aggregate. (**C–F**) The aggregation ability of each mutant was assessed and representative merged images were showed for each mutant, including R215H (C), V510M (D), R621H (E) and A637T (F). (**G**) Quantification of the aggregation assay shows that R215H mutation had significantly impaired aggregation compared with the wild-type, while V510M, R621H and A637T mutants did not show significant differences. $^{*}P < 0.05$, $^{**}P < 0.01$. The scale bar is 60 μm.

induced IPSCs in $3 \pm 3\%$ ($n = 24$) (Fig. 4C). On the other hand, there was no significant difference in the amplitudes of whole-cell GABA currents among all tested NLGN2 groups, suggesting that all four mutants did not affect the surface expression of $GABA_A$Rs in HEK 293T cells (Fig. 4D). Kinetic analysis of the IPSCs recorded in HEK 293T cells found no differences between wild-type and mutant NLGN2-expressing cells and they are similar to synaptic events recorded from neurons (data not shown). In summary, the R215H mutation abolished the synaptogenic activity of NLGN2 in promoting GABAergic synapse formation.

### The R215H mutant showed defects in trafficking and maturation

To understand the molecular mechanism underlying the incompetence of the R215H mutant in mediating cell adhesion and promoting GABAergic synaptogenesis, we examined the sub-cellular localization of the wild-type and the mutant NLGN2 proteins. HEK 293T cells were transfected individually with GFP or GFP tagged wild-type or mutant NLGN2. After 2-day expression, immunostaining against GFP (to enhance the signal of GFP tag) and the endoplasmic reticulum (ER) marker calnexin revealed that the R215H mutant was largely retained in the ER and showed decreased surface expression (Fig. 5C). In contrast, wild-type NLGN2 and the other three NLGN2 mutants showed high expression level on plasma membranes and less co-localization with calnexin (Figs 5B and 6).

Because NLGNs are highly glycosylated at the extracellular domain and glycosylation is essential for protein maturation (19,20), the ER retention of R215H suggested a possible defect in glycosylation and protein maturation. Indeed, immunoblotting against NLGN2 revealed that the wild-type NLGN2, mutants V510M, R621H and A637T all had two bands corresponding to mature and immature proteins, but the mutant R215H only had one band, likely representing an immature protein of lower molecular weight (Fig. 5D). Previous studies have shown that the difference in molecular weight between mature and immature NLGNs is caused by the addition of glycans (21–23). Therefore, the NLGN2 R215H mutant is a loss-of-function mutant that is largely retained in the ER and is deficient in post-translational modification and surface expression.

Clinical findings of the patient with the R215H mutation

The patient carrying the R215H mutation is a male with the age of 52 years at the time of interview. He was born in a family with two brothers and four sisters. His parents had
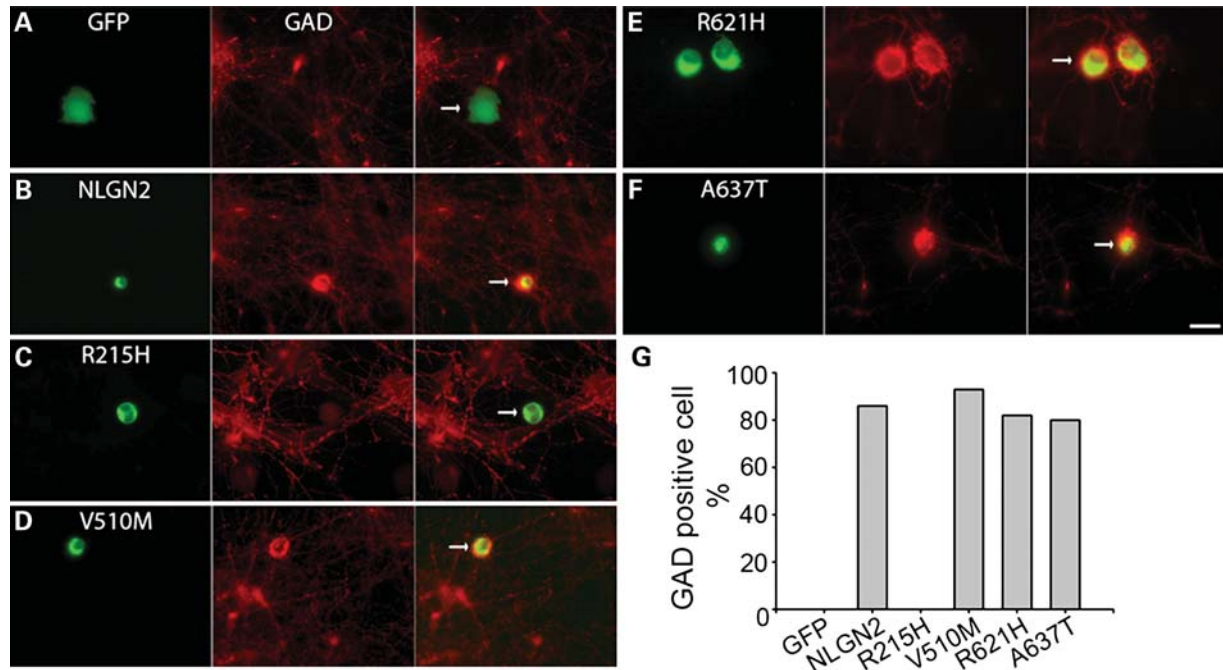
Figure 3. GABAergic synapse formation assay of four missense NLGN2 mutants. (**A**–**F**) Representative images showing the transfected HEK 293T cells (green) and immunostaining of GAD to visualize GABAergic terminals (Red). Cell transfected with GFP alone did not have GAD positive staining (A), while the wild-type NLGN2-expressing cell had positive GAD staining (B). Among four NLGN2 mutants (C–F), the R215H mutant did not have GAD positive staining. (**G**) Quantification confirms that the R215H mutant has no detectable GAD positive cells, while the other three mutants showed no differences in the counts of GAD positive cells compared the wild-type (GFP: 0 out of total 16 cells examined; wild-type NLGN2: 18/21; R215H: 0/27; V510M: 14/15; R621H: 14/17; A637T: 12/15). Arrows point to transfected HEK 293T cells in merged images. Scale bar, 10 μm.

passed away; there was no history of mental illness in this family except for the patient. He was born at full-term with uneventful pregnancy. The developmental history of the patient was unremarkable, except that he did not perform well academically in the elementary and junior high schools. At the age of 17 years, he started to present psychotic symptoms such as self-talking, self-laughing, auditory hallucination, delusion of persecution and violent and aggressive behavior. He was diagnosed with schizophrenia based on the Diagnostic and Statistical Manual of Mental Disorders, 4th edition (DSM-IV, American Psychiatric Association, 1994), and received antipsychotic drugs treatment. There was no history of illicit drug abuse, head injury or seizure attack in this patient. He responded well to the treatment with antipsychotic drugs; however, he did not comply well to the medication. Therefore, his psychotic symptoms relapsed every time when he stopped his medication. As a result, he was hospitalized to psychiatric wards several times due to the relapse of his symptoms. His social function deteriorated gradually throughout the years, and currently he still stayed in a chronic psychiatric hospital with the existence of residual psychotic symptoms. To investigate the genetic aspect of this mutation, we were able to obtain blood sample from one of his elder brothers who had no history of mental disorders. Sequencing data showed that the unaffected brother also carried the R215H mutation, suggesting the mutation was inherited from one of their parents. The absence of psychiatric symptoms of the elder brother indicates that the R215H mutation has incomplete penetrance. Since we were not able to collect DNA samples from all the family members for

genetic analysis, the penetrance of this mutation is unclear; hence, the clinical relevance of this mutation should be interpreted with caution.

DISCUSSION

In this study, we identified six missense rare mutations of the *NLGN2* gene in a sample of 584 schizophrenia patients and 549 control subjects from Taiwan after resequencing all the exonic regions and promoter region. Among these six mutations, four (R215H, V510M, R612H and A637T) were detected in patient group only, while two (P800L and A819S) were detected in both patient and control group. We found a tendency of the missense mutations over-represented in patient group compared with control group (8 of 584 versus 2 of 549), but the difference did not reach statistical significance ($P = 0.07$, Fisher's exact test), which might be due to the limited sample size of this study. *In silico* analysis predicted that both R215H and R612H mutations have probable damaging effects, but not the other four mutations.

In the functional characterization of these four missense mutations, we identified the R215H mutant as a loss-of-function mutant based on two lines of evidence: first, when expressed in HEK 293T cells, the R215H mutant cannot mediate cell aggregates with NRXN1β-expressing cells; second, the R215H mutant is incompetent to induce GABAergic synapse formation between HEK 293T cells and neurons as demonstrated by both immunocytochemistry and electrophysiology assays. Moreover, we demonstrated that
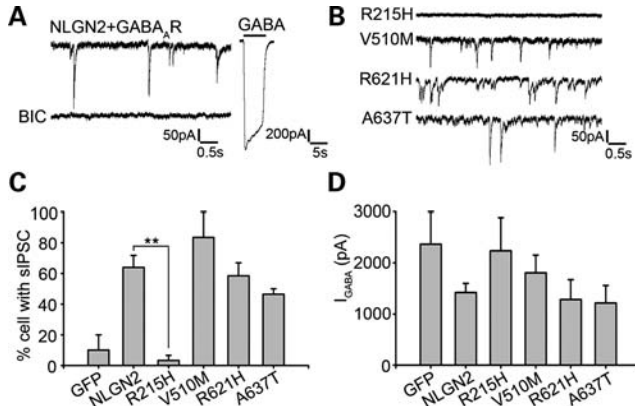
Figure 4. Electrophysiological activity assay of four missense NLGN2 mutants. (**A**) HEK 293T cells-expressing $GABA_AR$ and NLGN2 showed spontaneous activity after co-culturing with neurons, which was blocked by bicuculline (BIC). The right panel shows the whole cell GABA current after the application of 100 μM GABA. (**B**) Representative traces of whole-cell recording in HEK 293T cells expressing NLGN2 mutants. (**C**) Comparison of the percentages of HEK 293T cells showed spontaneous activity after co-transfection of $GABA_AR$ with each NLGN2 mutant. The R215H mutant had significant reduced percentage compared with the wild-type, while the other three mutants did not show significant differences from the wild-type (GFP: $10 \pm 10\%$; NLGN2: $64 \pm 8\%$; R215H: $3 \pm 3\%$; V510M: $84 \pm 14\%$; R621H: $59 \pm 9\%$; A637T: $47 \pm 4\%$). (**D**) Quantification of whole cell GABA currents showed no significant differences between each group. $**P < 0.01$.

the loss-of-function of R215H is caused by its deficiency in trafficking from the ER to the cell surface. Considering the importance of NLGN2 at GABAergic synapses, the R215H mutant may lead to impaired inhibitory circuit formation and contribute to the onset of schizophrenia. The other three mutations, V510M, R621H and A637T, behaved similar to the wild-type NLGN2 in this study, suggesting that their functional implications might be subtle and further study is necessary to determine their functional relevance.

Although many mutations in the *NLGN* and *NRXN* gene families have been identified in patients with psychiatric disorders, few of them have been functionally characterized. Our study of the R215H of NLGN2, together with previously reported R451C of NLGN3, R87W of NLGN4 and D396X of NLGN4 (5,23–25), provides strong evidence to indicate that mutations in the *NLGN* gene family are critically associated with neurodevelopmental disorders, including schizophrenia, autism and mental retardation. Our system of molecularly engineered GABAergic synapse has the advantage of blank background and easy manipulation, which could be broadly applied in characterizing human disease related mutants.

Arginine 215 is highly conserved among all human NLGNs and across species. Our imaging and biochemical data suggested that the R215H substitution undermines the surface expression and the maturation of NLGN2. Recently, De Jaco *et al.* (22) have shown that disease-related mutations in the α/β-hydrolase fold superfamily of proteins, including NLGNs, share common trafficking deficiencies. The prevalence of NLGN mutants causing ER retention (including R451C of NLGN3, R87W of NLGN4 and R215H of NLGN2) raises the possibility of applying pharmacological

chaperone to restore the surface expression of NLGN (26,27), since some mutant NLGNs, such as NLGN4 R87W, still binds NRXN and may promote synaptogenesis after reaching the membrane (23). Based on recently resolved structure of NLGN–NRXN complex and systematically mutational analysis study (28–30), Arginine 215 is located away from both NLGN dimerization and NLGN–NRXN binding interfaces. However, it is possible that the R215H substitution affects the NRXN-binding affinity of NLGN2 because the mutation of a distant aspartate (NLGN1 D271), not mutations of residues near interfaces, completely abolished the binding of NLGN1 to NRXN1β (30).

Following genetic association studies, several lines of *NLGN* transgenic mice have been generated in an effort to pinpoint the functional consequences of human *NLGN* mutations and set up animal models for human psychiatric disorders. Notably, the R451C mutant of *NLGN3* was originally discovered in two Swedish brothers, one with autism and the other with Asperger syndrome (31). Knock-in of the R451C mutant in mice resulted in autism-related impaired social interaction behaviors (25). Mice over-expressing NLGN1 or NLGN2 also had abnormal behaviors (32,33). As a loss-of-function mutation, the NLGN2 R215H mutation could decrease the formation or maturation of GABAergic synapses and alter the balance between neuronal excitation and inhibition which is essential for the normal cognitive function of the brain.

Acknowledging the complicated nature of psychiatric disorders including schizophrenia and autism, our discovery of schizophrenia-associated NLGN2 mutants supports the notion that mutations in synaptic proteins are highly associated with psychiatric disorders. As mutations of NLGN family genes were originally reported to be associated with autism in the literature, we evaluated carefully the psychiatric diagnosis of this patient. After reviewing his medical records and examining his mental status during this study, we did not find evidence to indicate that the patient co-morbid with autism spectrum disorder or mental insufficiency. In the genetic study of mutation, we found one of his elder brothers also carried this mutation, indicating that this mutation might inherit from one of their parents who had passed away. The mutation carrier brother has neither past history of psychiatric disorders nor present mental illness in this study, indicating that the R215H mutation is not fully penetrant. In view of genetic underpinnings of psychiatric disorders are complex and usually involve multiple genes and interactions with environmental factors, there might be the presence of modifying factors that determine the threshold of the clinical presentation in carriers of this mutation. In addition, since we were not able to collect DNA samples and evaluate the clinical phenotypes of all the family members, the penetrance and full picture of clinical presentations of this mutation are unclear. Hence, the clinical relevance of this mutation should be interpreted with caution. Future study using transgenic mouse models carrying these *NLGN* mutations is necessary to understand the functional consequence of these NLGN mutants *in vivo* and, most importantly, to elucidate whether and how they contribute to the etiology of psychiatric disorders.
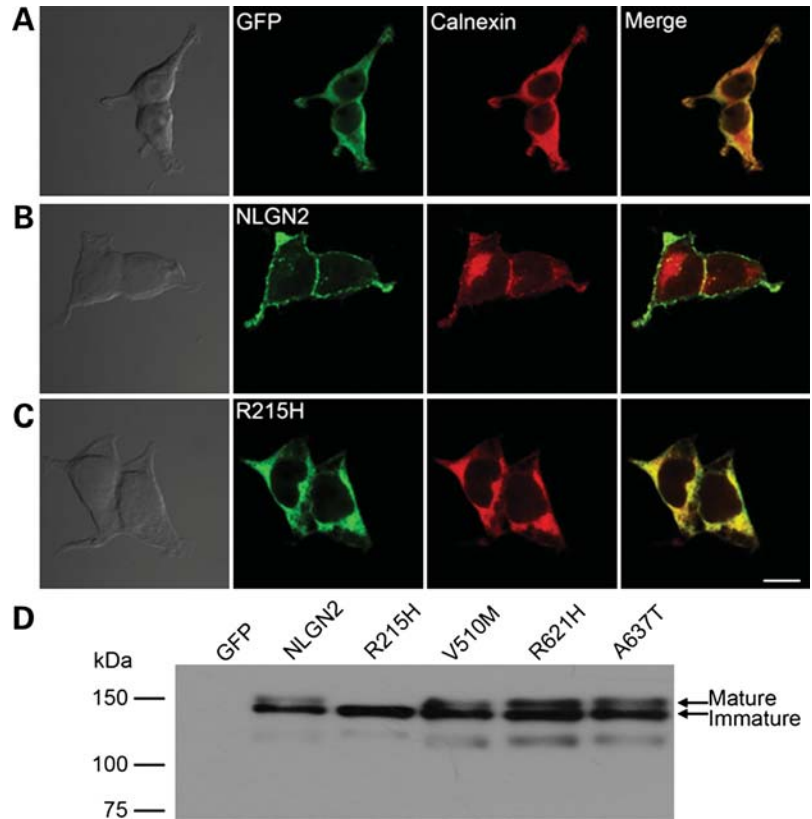
Figure 5. R215H mutant had deficiency in trafficking to cell surface and protein maturation. (**A**–**C**) Representative DIC and fluorescent images showing HEK 293T cells expressing GFP (A), wild-type NLGN2 (B) and R215H mutant (C), immunostained with antibodies against GFP (green) and the ER marker calnexin (red). As the wild-type NLGN2 showed robust surface expression (B), the R215H mutant was largely retained in the ER (C). Scale bar, 10 μm. (**D**) Immunoblot revealed that the R215H mutant showed only one band with low molecular weight, whereas the wild-type and the other three mutants all showed two bands.
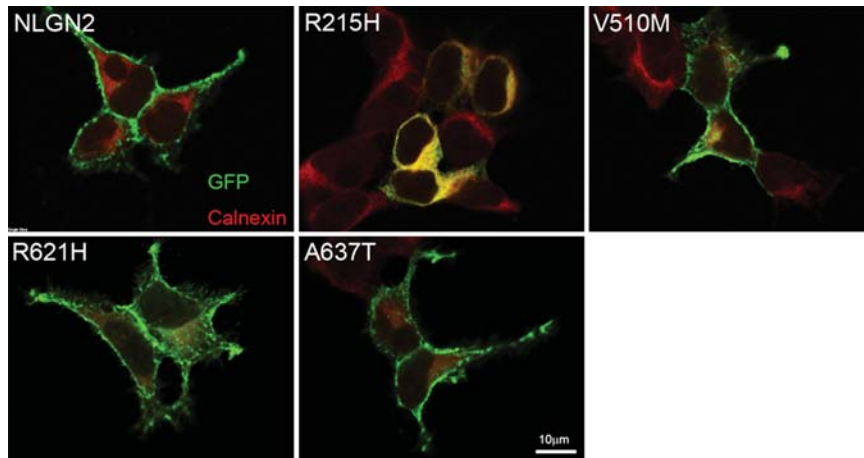
Figure 6. Expression of wild-type NLGN2 and NLGN2 mutants in HEK 293T cells showed only R215H had decreased surface expression and retained inside the ER. Immunostaining was performed with GFP (green) and calnexin (red) antibodies.

MATERIALS AND METHODS

Subjects

All subjects were Han Chinese from Taiwan. Patients fulfilling the diagnostic criteria of schizophrenia defined by the Diagnostic and Statistical Manual of Mental Disorders (DSM-IV) were recruited into this study. The diagnosis of schizophrenia was based on clinical interview and review of medical records by senior psychiatrists with consensus. Exclusion criteria include psychosis due to general medical condition, substance-related psychosis and mood disorder with psychotic features. Non-psychotic controls were recruited from a

medical center's Department of Family Medicine located in eastern Taiwan. The study was approved by the Institution Review Board and written informed consent was obtained after the procedures were fully explained. The patient group comprised 584 schizophrenic patients (362 males, 222 females, mean age = 43 years), while the control group comprised 549 subjects (242 males, 307 females, mean age = 43 years). Genomic DNA was prepared from peripheral blood cells according to standard protocols.

PCR amplification

Optimal PCR primer sequences were generated to amplify all the exons and the putative promoter region of the *NLGN2* gene using Primer3 (http://frodo.wi.mit.edu/primer3/). Primer sequences, optimal annealing temperatures and size of each amplicon are listed in Supplementary Material, Table S1. In a standard reaction, 100 ng of genomic DNA was amplified in a reaction volume of 20 µl containing 1 µM sense and antisiense primer, 0.2 mM dNTP, 50 mM KCl, 1.5 mM MgCl$_2$, 0.1% vol/vol Triton X-100, 10 mM Tris–HCl (pH = 9.0) and 2.5 U *Taq* polymerase. PCR cycling program consisted of an initial template denaturation at 95°C for 5 min, followed by 30 cycles of 95°C for 1 min, optimal annealing temperature for 1 min and 72°C for 1 min. PCR was performed in a PTC-200 Peltier Thermal Cycler (MJ Research, Watertown, MA, USA).

Direct PCR autosequencing

After PCR amplification, aliquots of PCR products were processed using a PCR Pre-Sequencing Kit (USB Corp. Cleveland, OH, USA) to remove residual primers and dNTPs following the manufacturer's protocol. The purified PCR products were subjected to direct sequencing using an ABI Prism™ BigDye™ Terminator Cycle Sequencing Ready Reaction Kit Version 3.1, and an ABI autosequencer 3730 (Perkin Elmer Applier Biosystem, Foster City, CA, USA) according to manufacturer's protocol. All the variants were verified by repeated PCR and sequencing in both directions.

Restriction fragment length polymorphism analysis

Two missense mutations (R215H, V510M) were also confirmed using PCR-based RFLP analysis. In brief, aliquots of PCR products of exon 3 and exon 6 of the *NLGN2* gene were digested with *Bcc*I and *Sph*I overnight at 37°C incubation, respectively. The digested PCR products were subjected to 2% agarose gel electrophoresis. For R215H mutation, the G allele (R) yielded 203 and 256 bp PCR fragments, while the A allele (H) yielded 67, 189 and 203 bp PCR fragments. For V510M mutation, the A allele (M) yielded 232 and 321 bp PCR fragments, while the G allele (V) remained uncut (553 bp).

Statistical analysis

The differences of frequency of rare mutations between patient and control groups were assessed using Fisher's exact test with the significance level at 0.05 (one-tailed).

In silico analysis

Prediction of potential deleterious effects of missense mutations detected in the *NLGN2* gene was performed using the software tools PolyPhen-2 (http://genetics.bwh.harvard.edu/pph2/) and SIFT (http://sift.jcvi.org/).

Construction of expression plasmids

The wild-type cDNA of the human *NLGN2* gene was obtained by PCR amplification of human brain Marathon-Ready cDNA (ClonTech Laboratories, Inc., USA) using primer NLGN2F (5′-CCCGATCAGCATGTGGCTCC-3′) and primer NLGN2R (5′-CTACCCGAGTGGTGGAGTGG-3′). The PCR amplicon (2516 bp) was cloned into the pcDNA3.1/CT-GFP-TOPO vector (Invitrogen, CA, USA) and its authenticity was verified by sequencing. This wild-type cDNA construct was as a template for the construction of mutant constructs. The mutant construct NLGN2-Arg215His-GFP was obtained using megaprimer method (34). In brief, the primer 1 (5'-CGCAAATGGGCGGTAGGCGTG-3′) and the primer 2 (5′-CACCCCAAGA**T**GGTAGTTGA-3′) that contained the mutant sequence were used to obtain a PCR amplicon of 858 bp. After purification, aliquots of the amplicon were used as a megaprimer to obtain an amplicon of 2094 bp with the primer 3 (5′-CGGCCAGCGCGTGGCGTAGG-3′) that contained the *Pfl*MI restriction recognition site. After digestion with the *Kpn*I and *Pfl*MI, the amplicon was subcloned into the wild-type NLGN2-cDNA. The mutant type NLGN2-V510M-GFP was constructed by the replacement of wild-type allele with the mutant amplicon by PCR amplification of the mutant cDNA from the lymphoblastoid cells of the patient using the sense primer (5′-AGCGCCTTTGACTTCACTGT-3′) and antisense primer (5′-CACCCACCCCCTATACCCGA-3′) that contained the *Pfl*MI recognition site sequences. For mutant type NLGN2-R621H-GFP, the mutant PCR products were obtained by primer NLGN2-R621H-sense (5′-AGCGCCTTTGACTTCACTGT-3′) and the NLGN2-R621H-antisense (5′-CCAGCGCGTGGCGTAGGGAGGCAGG**T**GCGT-3′). The amplicon was digested with *Pfl*MI and cloned into the pcDNA3.1/CT-GFP vector. For mutant NLGN2-A637T-GFP, the PCR products were obtained by the NLGN2-A637T-sense primer (5′-CCACGCGCTGGCCGCCTCGTCCCCCCGCTGGCA**C**CC-3′) and the reverse primer (5′-GGGTAAGCTTTCCGTATGTAGC-3′). The amplicon was digested with *Pfl*MI and *Xba*I and subcloned into the pcDNA3.1/CT-GFP vector. The authenticity of all the constructs was verified by sequencing.

Cell culture

Hypothalamic neurons and human embryonic kidney (HEK) 293T cells were cultured as previously described (18). HEK 293T cells were co-transfected with GABA$_A$ receptors (α2β3γ2) and wild-type or mutant human NLGN2 plasmids by calcium phosphate method (35). After 24 h of transfection, HEK 293T cells were trypsinized and plated on top of 10–12 DIV hypothalamic cultures and co-cultured for 2–3 days before functional analysis. Typically, each experiment was repeated in at least three different batches of cultures.

Cell aggregation assay

To investigate the interaction between mutant NLGN2 and NRXN, we expressed each protein separately in different HEK 293T cells and then mixed the cells together to perform cell aggregation assay. All NLGN2 plasmids were GFP-tagged. DsRed was co-transfected to visualize NRXN1β (Gift from Dr Ann Marie Craig) expressing cells. One day after transfection, the same amount of NRXN1β transfected cells were trypsinized and mixed with GFP, GFP-NLGN2 or GFP-NLGN2 mutant transfected HEK 293T cells. Mixtures were incubated at 37°C with gentle rotation for 90 min and plated in 24-well plate for aggregation assay. Fluorescent images of 3–5 fields were chosen randomly from each well. Particles were counted by ImageJ software. The percentage of aggregation was determined by $A = (N_{GFP} + N_{RFP} - N_{mix})/(N_{GFP} + N_{RFP})$, where A is degree of aggregation, N_{GFP} the number of GFP-labeled particles, N_{RFP} the number of RFP-labeled particles and N_{mix} is total number of particles in the GFP and RFP merged images. If no aggregation, $N_{mix} = N_{GFP} + N_{RFP}$ and $A = 0$. If all cells aggregate together into one particle, $N_{mix} = 1$. The final aggregation index was normalized by A_{90min}/A_{0min}. Data from three independent experiments were presented as average ± standard error.

Immunofluorescence analyses

Cells were first fixed at room temperature in 4% paraformaldehyde for 10 min and permeabilized with 0.2% Triton X-100 for 5 min. The cells were incubated with primary antibody in phosphate buffered saline (PBS) with 10% donkey serum overnight at 4°C or 2 h at room temperature and then incubated with secondary antibody at room temperature for 45 min. The average intensity of GAD signal was measured by ImageJ. Two-fold increase of the GAD signal compared with non-transfected HEK 293T cells was set as the threshold to determine whether HEK 293T cells had positive GAD puncta. The following primary antibodies were used: GAD6 (mouse monoclonal, 1:100; Developmental Studies Hybridoma Bank City, Iowa City, IA, USA), calnexin (mouse monoclonal, BD Biosciences Transduction Laboratories, San Jose, CA, USA), GFP (chicken polyclonal, Abcam, Cambridge, MA, USA). Alexa Fluor 488 and 546 conjugated secondary antibodies were purchased from Molecular Probes (Eugene, OR, USA).

Electrophysiology

Whole-cell patch clamp recordings were performed on transfected HEK 293T cells after 2–3 days of co-culture with hypothalamus neurons, as previously described (18). Briefly, Multiclamp 700A amplifier and pClamp software were used for acquiring data (sampling at 5 kHz and filtered at 1 kHz). Data analysis was performed using Clampfit and Synaptosoft. The normal recording solution contained (in mM): 128 NaCl, 30 glucose, 25 HEPES, 5 KCl, 2 CaCl$_2$ and 1 MgCl$_2$ (320 mOsm, adjusted to pH 7.3 with NaOH). The pipette solution contained (in mM): 135 KCl, 10 Tris–phosphocreatine, 2 EGTA, 10 HEPES, 4 MgATP, 0.5 Na$_2$GTP (~300 mOsm,

adjusted to pH 7.3 with KOH). The membrane potential was clamped at −70 mV. Series resistance was typically 10–25 MΩ. The analyzed data were expressed as mean ± standard errors. The Student's *t*-test was employed for statistical analysis.

Western blot

HEK 293T cells in six-well plates were transfected using polyethylenimine (Polysciences, Inc., Warrington, PA, USA). After 2-day expression, cells were washed twice with cold PBS and re-suspended in 300 μl lysis buffer containing 20 mM HEPES, 1% Triton X-100, 0.1 mM EDTA, 2 mM CaCl$_2$, 1 mM MaCl$_2$ and 50 mM NaCl with protease inhibitors, PMSF and phosphatase inhibitors (pH 7.3 with NaOH). After 1 h incubation at 4°C, supernatants were harvested by centrifugation (12 000*g*, 30 min). Samples were boiled at 95°C for 10 min with 1% β-mercaptoethanol and SDS loading buffer (Invitrogen, Carlsbad, CA, USA). Rabbit polyclonal antibody against NLGN2 was purchased from Synaptic Systems (Gottingen, Germany).

SUPPLEMENTARY MATERIAL

Supplementary Material is available at *HMG* online.

REFERENCES

1. Cardno, A.G. and Gottesman, I.I. (2000) Twin studies of schizophrenia: from bow-and-arrow concordances to star wars Mx and functional genomics. *Am. J. Med. Genet.*, **97**, 12–17.
2. Lewis, D.A. and Gonzalez-Burgos, G. (2006) Pathophysiologically based treatment interventions in schizophrenia. *Nat. Med.*, **12**, 1016–1022.
3. McGlashan, T.H. and Hoffman, R.E. (2000) Schizophrenia as a disorder of developmentally reduced synaptic connectivity. *Arch. Gen. Psychiatry*, **57**, 637–648.
4. Sudhof, T.C. (2008) Neuroligins and neurexins link synaptic function to cognitive disease. *Nature*, **455**, 903–911.
5. Chih, B., Engelman, H. and Scheiffele, P. (2005) Control of excitatory and inhibitory synapse formation by neuroligins. *Science*, **307**, 1324–1328.
6. Chubykin, A.A., Atasoy, D., Etherton, M.R., Brose, N., Kavalali, E.T., Gibson, J.R. and Sudhof, T.C. (2007) Activity-dependent validation of excitatory versus inhibitory synapses by neuroligin-1 versus neuroligin-2. *Neuron*, **54**, 919–931.
7. Futai, K., Kim, M.J., Hashikawa, T., Scheiffele, P., Sheng, M. and Hayashi, Y. (2007) Retrograde modulation of presynaptic release probability through signaling mediated by PSD-95–neuroligin. *Nat. Neurosci.*, **10**, 186–195.

8. Gottmann, K. (2008) Transsynaptic modulation of the synaptic vesicle cycle by cell-adhesion molecules. *J. Neurosci. Res.*, **86**, 223–232.

9. Missler, M., Zhang, W., Rohlmann, A., Kattenstroth, G., Hammer, R.E., Gottmann, K. and Sudhof, T.C. (2003) Alpha-neurexins couple Ca2+ channels to synaptic vesicle exocytosis. *Nature*, **423**, 939–948.

10. Dean, C. and Dresbach, T. (2006) Neuroligins and neurexins: linking cell adhesion, synapse formation and cognitive function. *Trends Neurosci.*, **29**, 21–29.

11. Goldstein, G., Minshew, N.J., Allen, D.N. and Seaton, B.E. (2002) High-functioning autism and schizophrenia: a comparison of an early and late onset neurodevelopmental disorder. *Arch. Clin. Neuropsychol.*, **17**, 461–475.

12. Sheitman, B.B., Kraus, J.E., Bodfish, J.W. and Carmel, H. (2004) Are the negative symptoms of schizophrenia consistent with an autistic spectrum illness? *Schizophr. Res.*, **69**, 119–120.

13. Kirov, G., Gumus, D., Chen, W., Norton, N., Georgieva, L., Sari, M., O'Donovan, M.C., Erdogan, F., Owen, M.J., Ropers, H.H. *et al.* (2008) Comparative genome hybridization suggests a role for NRXN1 and APBA2 in schizophrenia. *Hum. Mol. Genet.*, **17**, 458–465.

14. Kirov, G., Rujescu, D., Ingason, A., Collier, D.A., O'Donovan, M.C. and Owen, M.J. (2009) Neurexin 1 (NRXN1) deletions in schizophrenia. *Schizophr. Bull.*, **35**, 851–854.

15. Sand, P., Langguth, B., Hajak, G., Perna, M., Prikryl, R., Kucerova, H., Ceskova, E., Kick, C., Stoertebecker, P. and Eichhammer, P. (2006) Screening for Neuroligin 4 (NLGN4) truncating and transmembrane domain mutations in schizophrenia. *Schizophr. Res.*, **82**, 277–278.

16. Walsh, T., McClellan, J.M., McCarthy, S.E., Addington, A.M., Pierce, S.B., Cooper, G.M., Nord, A.S., Kusenda, M., Malhotra, D., Bhandari, A. *et al.* (2008) Rare structural variants disrupt multiple genes in neurodevelopmental pathways in schizophrenia. *Science*, **320**, 539–543.

17. Lewis, D.A., Hashimoto, T. and Volk, D.W. (2005) Cortical inhibitory neurons and schizophrenia. *Nat. Rev. Neurosci.*, **6**, 312–324.

18. Dong, N., Qi, J. and Chen, G. (2007) Molecular reconstitution of functional GABAergic synapses with expression of neuroligin-2 and GABAA receptors. *Mol. Cell. Neurosci.*, **35**, 14–23.

19. Hebert, D.N., Garman, S.C. and Molinari, M. (2005) The glycan code of the endoplasmic reticulum: asparagine-linked carbohydrates as protein maturation and quality-control tags. *Trends Cell Biol.*, **15**, 364–370.

20. Hoffman, R.C., Jennings, L.L., Tsigelny, I., Comoletti, D., Flynn, R.E., Sudhof, T.C. and Taylor, P. (2004) Structural characterization of recombinant soluble rat neuroligin 1: mapping of secondary structure and glycosylation by mass spectrometry. *Biochemistry*, **43**, 1496–1506.

21. De Jaco, A., Comoletti, D., Kovarik, Z., Gaietta, G., Radic, Z., Lockridge, O., Ellisman, M.H. and Taylor, P. (2006) A mutation linked with autism reveals a common mechanism of endoplasmic reticulum retention for the alpha,beta-hydrolase fold protein family. *J. Biol. Chem.*, **281**, 9667–9676.

22. De Jaco, A., Lin, M.Z., Dubi, N., Comoletti, D., Miller, M.T., Camp, S., Ellisman, M., Butko, M.T., Tsien, R.Y. and Taylor, P. (2010) Neuroligin trafficking deficiencies arising from mutations in the alpha/beta-hydrolase fold protein family. *J. Biol. Chem.*, **285**, 28674–28682.

23. Zhang, C., Milunsky, J.M., Newton, S., Ko, J., Zhao, G., Maher, T.A., Tager-Flusberg, H., Bolliger, M.F., Carter, A.S., Boucard, A.A. *et al.* (2009) A neuroligin-4 missense mutation associated with autism impairs neuroligin-4 folding and endoplasmic reticulum export. *J. Neurosci.*, **29**, 10843–10854.

24. Comoletti, D., De Jaco, A., Jennings, L.L., Flynn, R.E., Gaietta, G., Tsigelny, I., Ellisman, M.H. and Taylor, P. (2004) The Arg451Cys-neuroligin-3 mutation associated with autism reveals a defect in protein processing. *J. Neurosci.*, **24**, 4889–4893.

25. Tabuchi, K., Blundell, J., Etherton, M.R., Hammer, R.E., Liu, X., Powell, C.M. and Sudhof, T.C. (2007) A neuroligin-3 mutation implicated in autism increases inhibitory synaptic transmission in mice. *Science*, **318**, 71–76.

26. Chih, B., Afridi, S.K., Clark, L. and Scheiffele, P. (2004) Disorder-associated mutations lead to functional inactivation of neuroligins. *Hum. Mol. Genet.*, **13**, 1471–1477.

27. Morello, J.P., Petaja-Repo, U.E., Bichet, D.G. and Bouvier, M. (2000) Pharmacological chaperones: a new twist on receptor folding. *Trends Pharmacol. Sci.*, **21**, 466–469.

28. Arac, D., Boucard, A.A., Ozkan, E., Strop, P., Newell, E., Sudhof, T.C. and Brunger, A.T. (2007) Structures of neuroligin-1 and the neuroligin-1/neurexin-1 beta complex reveal specific protein-protein and protein-Ca2+ interactions. *Neuron*, **56**, 992–1003.

29. Fabrichny, I.P., Leone, P., Sulzenbacher, G., Comoletti, D., Miller, M.T., Taylor, P., Bourne, Y. and Marchot, P. (2007) Structural analysis of the synaptic protein neuroligin and its beta-neurexin complex: determinants for folding and cell adhesion. *Neuron*, **56**, 979–991.

30. Reissner, C., Klose, M., Fairless, R. and Missler, M. (2008) Mutational analysis of the neurexin/neuroligin complex reveals essential and regulatory components. *Proc. Natl Acad. Sci. USA*, **105**, 15124–15129.

31. Jamain, S., Quach, H., Betancur, C., Rastam, M., Colineaux, C., Gillberg, I.C., Soderstrom, H., Giros, B., Leboyer, M., Gillberg, C. *et al.* (2003) Mutations of the X-linked genes encoding neuroligins NLGN3 and NLGN4 are associated with autism. *Nat. Genet.*, **34**, 27–29.

32. Dahlhaus, R., Hines, R.M., Eadie, B.D., Kannangara, T.S., Hines, D.J., Brown, C.E., Christie, B.R. and El-Husseini, A. (2010) Overexpression of the cell adhesion protein neuroligin-1 induces learning deficits and impairs synaptic plasticity by altering the ratio of excitation to inhibition in the hippocampus. *Hippocampus*, **20**, 305–322.

33. Hines, R.M., Wu, L., Hines, D.J., Steenland, H., Mansour, S., Dahlhaus, R., Singaraja, R.R., Cao, X., Sammler, E., Hormuzdi, S.G. *et al.* (2008) Synaptic imbalance, stereotypies, and impaired social interactions in mice with altered neuroligin 2 expression. *J. Neurosci.*, **28**, 6055–6067.

34. Tyagi, R., Lai, R. and Duggleby, R. (2004) A new approach to 'megaprimer' polymerase chain reaction mutagenesis without an intermediate gel purification step. *BMC Biotechnol.*, **4**, 2.

35. Jiang, M. and Chen, G. (2006) High Ca2+-phosphate transfection efficiency in low-density neuronal cultures. *Nat. Protoc.*, **1**, 695–700.